the corresponding chloride, which was identical with the cross-coupling product obtained above in GLC and ^{1}H NMR.

Coupling Reaction of 1 with an Organozinc. To a flask containing $ZnCl_2$ (137 mg, 1 mmol) in dry ether (4 mL) was added butyllithium (0.62 mL of a 15% hexane solution, 1 mmol) at 0 °C under an atmosphere of nitrogen, and the mixture was stirred for 30 min. After exchange of the solvent from ether to dichloromethane (4 mL) as before, **1a** (170 mg, 1 mmol) was added and this mixture was stirred for 21 h at room temperature. The same workup and purification as in the Grignard case gave **3** in 45% yield. Similarly, **12** was obtained in 30% yield from **1b** and phenyllithium.

Registry No. **1a**, 935-56-8; **1b**, 768-90-1; **1c**, 768-93-4; **2**, 281-23-2; **3**, 14449-41-3; **4**, 88458-84-8; **5**, 112298-59-6; **6**, 770-69-4; **7**, 768-91-2; **8**, 20440-81-7; **9**, 22922-62-9; **10**, 112298-60-9; **11**, 112298-61-0; **12**, 780-68-7; **13**, 1974-86-3; **14**, 2245-43-4; **15**, 57822-52-3; **16**, 112298-62-1; **17**, 112298-63-2; **18a**, 507-20-0; **18b**, 507-19-7; **19**, 17314-92-0; **20**, 63238-62-0; **21**, 63213-06-9; **22**, 624-96-4; **23**, 112319-77-4; $CH_3(CH_2)_3MgCl$, 693-04-9; $Ph(CH_2)_2MgCl$, 90878-19-6; $C_5H_9CH_2MgCl$, 108697-83-2; CH_3CH_2MgBr, 925-90-6; CH_3MgI, 917-64-6; $C(CH_3)_3MgCl$, 677-22-5; $CH_2{=}CHCH_2MgCl$, 2622-05-1; $CH_3CH{=}CHCH_2MgCl$, 6088-88-6; $CH_3(CH_2)_3MgBr$, 693-03-8; C_6H_5MgBr, 100-58-3; $3\text{-}CH_3C_6H_4MgBr$, 28987-79-3; $4\text{-}BrC_6H_4MgBr$, 18620-02-5; $C_{10}H_7MgBr$, 703-55-9; $CH_3(CH_2)_3MgI$, 1889-20-9; $C_6H_5(CH_2)_2MgBr$, 3277-89-2; 1-heptynylmagnesium bromide, 61307-38-8; 5-hexenylmagnesium bromide, 30043-41-5; cinnamylmagnesium chloride, 51800-74-9; butylzinc chloride, 42930-39-2; butyllithium, 109-72-8; 3-indolylmagnesium bromide, 7058-69-7; phenyllithium, 591-51-5.

Geometry of Porphyrin–Porphyrin Interactions

Philip Leighton,† J. A. Cowan,† Raymond J. Abraham,‡ and Jeremy K. M. Sanders*†

University Chemical Laboratory, Lensfield Road, Cambridge CB2 1EW, United Kingdom, and Robert Robinson Laboratories, University of Liverpool, P. O. Box 147, Liverpool L69 3BX, United Kingdom

Received September 9, 1987

NMR, UV/visible absorption, and fluorescence studies on two free base porphyrin cofacial dimers and on their dizinc derivatives are reported. In the free-base molecules, characteristic upfield chemical shifts induced at the protons and carbons of one porphyrin moiety by the ring current of the other porphyrin moiety are interpreted in terms of an offset stacked geometry; this geometry is virtually unchanged by insertion of zinc. It is suggested that the observed offset geometry is a fundamental property of the porphyrin–porphyrin interaction, being found in solution and solid state, in restrained porphyrin dimers, and in aggregates of unrestrained monomers. It is further suggested that these cofacial dimers are good models for the study of porphyrin–porphyrin aggregation.

It has been known for many years that porphyrins in solution tend to aggregate,[1-3] but we understand remarkably little of the nature or geometry of porphyrin–porphyrin interactions. There is a substantial amount of evidence to suggest that porphyrins prefer to stack in an offset manner rather than with one molecule directly over another,[3-7] but this evidence is too fragmentary to enable any firm conclusions to be drawn either about the fundamental geometry of the porphyrin–porphyrin interaction or about the role (if any) of a central metal ion. Three types of interaction have been previously proposed in connection with porphyrin aggregation:[3] (i) free-base porphyrins aggregate via a weak π–π interaction; (ii) some metalloporphyrins exhibit a stronger metal–π interaction that can be abolished by ligand binding to the metal; and (iii) a strong metal–side chain binding. The latter is particularly marked in magnesium-containing porphyrins and is not considered further in this paper.

We now present NMR, UV/visible absorption, and fluorescence results for a series of free base and metalated porphyrin cofacial dimers that elucidate several aspects of porphyrin aggregation chemistry. In particular, we demonstrate (a) that these dimers exhibit a preferred offset geometry in solution, (b) that this geometry is accompanied by strong electronic interaction, and (c) that the *geometry* of the interaction is not necessarily or significantly affected by the presence of a central metal ion but that the *strength* of the interaction may be affected. Finally, we suggest, on the basis of published results on other compounds, that these geometries and conclusions are a general property of the porphyrin–porphyrin interaction.

Most of the results described here have been obtained by using the meso form of the dimer **1** and its dizinc derivative Zn_2-**1**; some less detailed, but corroborative, results are also reported for **2** and Zn_2-**2**. These molecules have been designed such that they are adequately constrained to encourage intramolecular interaction and sufficiently flexible to be able to fold into a favorable conformation for porphyrin–porphyrin interaction. In addition, Zn_2-**1** is sufficiently loose that the two faces can be pried apart by manipulation of its coordination chemistry.

Our approach in this work has been described in detail very recently[8] so we summarize it here only briefly. The geometrical dependence of the ring-current shifts induced by porphyrins is well-known; it is therefore a relatively simple matter to interpret the shifts observed in a porphyrin cofacial dimer in terms of the relative disposition of the two component macrocycles. Similarly, the ap-

† University of Cambridge.
‡ University of Liverpool.

(1) White, W. I. In *The Porphyrins*; Dolphin, D., Ed; Academic: New York, 1978; Vol. V, p 303.
(2) Scheer, H. In *The Porphyrins*; Dolphin, D., Ed.; Academic: New York, 1978; Vol. II, p 1.
(3) (a) Abraham, R. J.; Eivazi, F.; Pearson, H.; Smith, K. M. *J. Chem. Soc., Chem. Commun.* **1976**, 698 and 699. (b) Abraham, R. J.; Fell, S. C. M.; Pearson, H.; Smith, K. M. *Tetrahedron* **1979**, *35*, 1759.
(4) Snyder, R. V.; La Mar, G. N. *J. Am. Chem. Soc.* **1977**, *99*, 7178.
(5) Eaton, S. S.; Eaton, G. R.; Chang, C. K. *J. Am. Chem. Soc.* **1985**, *107*, 3177.
(6) Abraham, R. J.; Smith, K. M. *J. Am. Chem. Soc.* **1983**, *105*, 5734.
(7) Hatada, M. H.; Tulinsky, A.; Chang, C. K. *J. Am. Chem. Soc.* **1980**, *102*, 7115 and **1981**, *103*, 5623.
(8) Abraham, R. J.; Leighton, P.; Sanders, J. K. M. *J. Am. Chem. Soc.* **1985**, *107*, 3472.

0022-3263/88/1953-0733$01.50/0

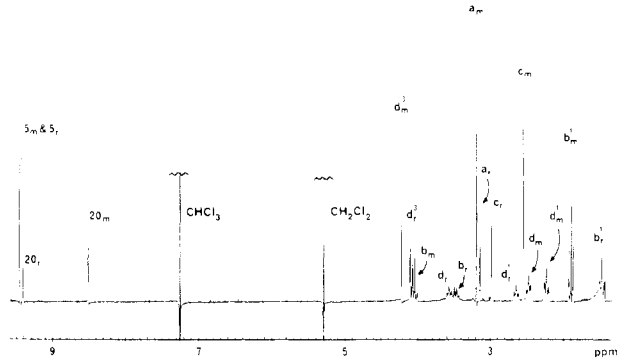

Figure 1. ^{1}H NMR spectrum (250 MHz) of 1 in $CDCl_3$ solution. Signals due to meso or racemic isomers are labeled m or r as appropriate.

pearance of exciton coupling is good evidence for the electronic interaction of two proximate π-systems.[9]

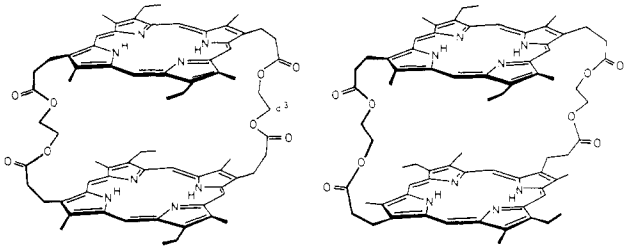

meso-1 racemic-1

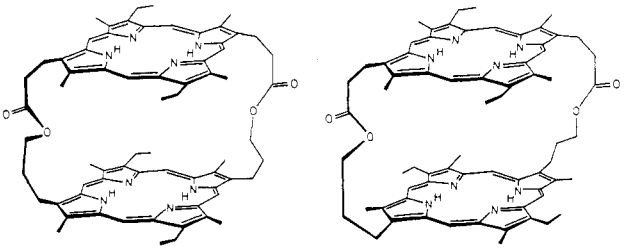

syn-2 anti-2

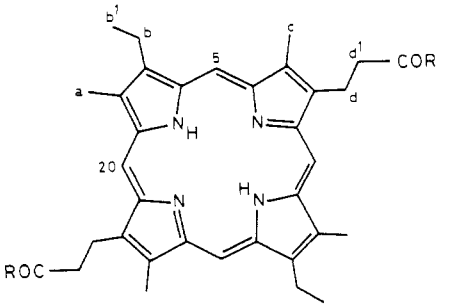

3: R = Cl

4: R = OCH_2CH_2OH

5: R = OMe

Results

Spectrum Assignments in Free-Base Dimers. The "symmetrical" dimer 1 was prepared by a straightforward extension of our previous syntheses of bridged and dimeric porphyrins.[10] High-dilution reaction of mesoporphyrin II bis(acid chloride), 3, with ethylene glycol in the presence of 4-(*N*,*N*-dimethylamino)pyridine as catalyst gave the diol, 4, in 43% yield; condensation of 4 with a further mole of 3 under similar conditions gave 1 in a yield of 9.7% (not optimized).

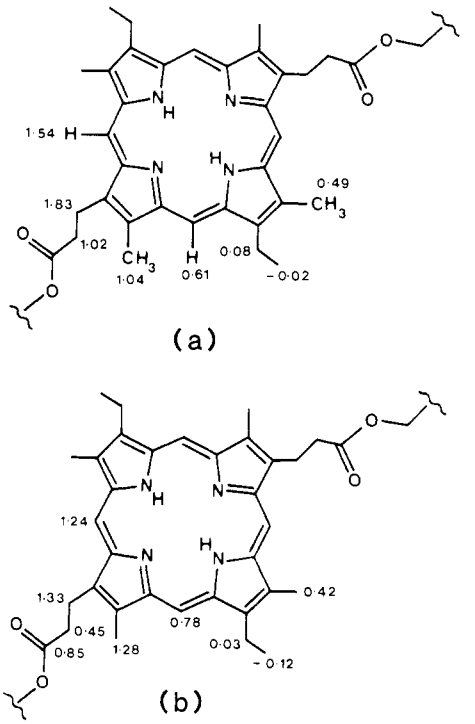

Figure 2. Upfield ring-current shifts (ppm) in *meso*-1 relative to 5: (a) ^{1}H shifts, (b) ^{13}C shifts.

Dimer 1 can exist as either meso or racemic isomers, which arise because there are two ways for the second porphyrin to lie on the first: the meso form has methyl on methyl, while the racemic form has methyl on ethyl. In principle, the two isomers may be interconverted by rotation of a porphyrin through the cavity, but this occurs slowly on the NMR chemical shift time scale, and both isomers are observed, in a 2:1 ratio, in NMR spectra of the synthetic product. We made no attempt to separate the two isomers, which moved as a single spot on thin-layer chromatography. In both dichloromethane-d_2 and 1,1,2,2-tetrachloroethane-d_2 there was much signal overlap between the ^{1}H signals of each isomer, but in chloroform-*d* they are well dispersed (Figure 1). The most remarkable feature of these spectra is the appearance of meso proton signals around 8 ppm: in monomeric porphyrins such as 5, they generally resonate around 10 ppm. This unusual shift provides the first clue of a specific geometry.

COSY and NOE difference spectra[11] (not shown) on the isomer mixture allowed unambiguous assignments to be made for all the peaks for both isomers with the exception of the two propionate triplets of the major isomer. Each was shifted so much that the usual assignment relying on chemical shift became unreliable. With one assignment, the upfield ring current induced shifts (relative to 5) were 1.83 and 1.02 ppm, while with reversed assignments they were 2.13 and 0.72 ppm. The former seems more reasonable and is supported by the observed NOEs to the adjacent meso proton: 3.7% for the triplet assigned to H_d and

(9) Kasha, M.; Rawls, H. R.; El-Bayoumi, M. A. *Pure Appl. Chem.* **1965**, *11*, 371.

(10) (a) Leighton, P.; Sanders, J. K. M. *J. Chem. Soc., Perkin Trans. 1* **1987**, 2385. (b) Cowan, J. A.; Sanders, J. K. M. *J. Chem. Soc., Perkin Trans. 1* **1987**, 2395. (c) Hunter, C. A.; Meah, M. N.; Sanders, J. K. M., in preparation.

(11) Sanders, J. K. M.; Hunter, B. K. *Modern NMR Spectroscopy*; Oxford University: Oxford, 1987.

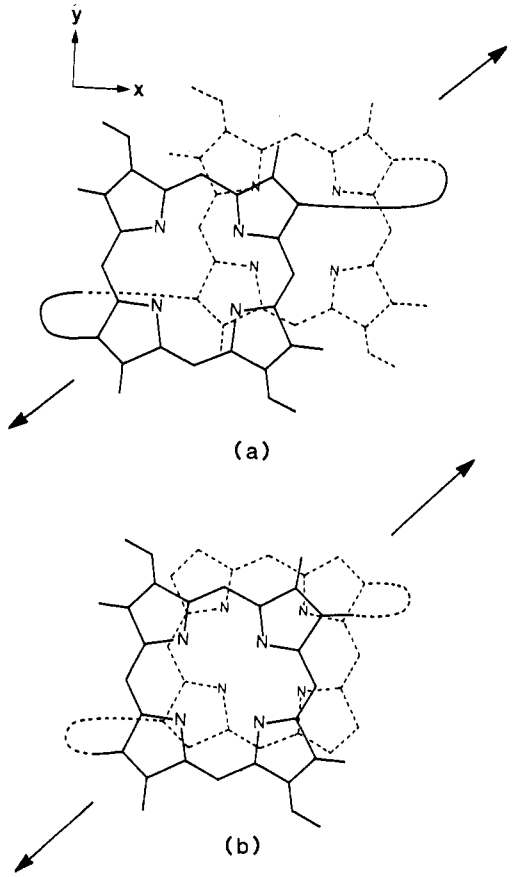

Figure 3. Cross-plane motions and calculated geometries for (a) *meso*-**1** and (b) the two isomers of **2**.

1.7% for $H_{d'}$. Figure 2(a) summarizes the ring current induced shifts, relative to **5**, found in the ^1H spectrum of the major isomer of **1**. It is noteworthy that in the major isomer a characteristic pattern of large shifts is found in only one part of the structure. In the other isomer a smaller, general upfield trend is apparent (see Experimental Section for details). In the NOE difference experiments, *no* saturation transfer between the isomers was observed, even at elevated temperatures; this places an upper limit of ca. 1 s^{-1} for the interconversion rate.

We had previously assigned the ^1H and ^{13}C (protonated carbons) spectra of **5** rigorously by using a combination of one-dimensional ^1H–^1H NOE and two-dimensional ^1H–^{13}C correlation experiments.[12] Using as a guide the ^{13}C shifts in **5** and the characteristic pattern of ^1H ring-current shifts in the major isomer of **1**, we were able to assign unambiguously the protonated carbons in the major isomer; these results are summarized in Figure 2(b) in the form of ring current induced shifts from **5**. This was not possible for the minor isomer, as the ^{13}C signals displayed the same general upfield shifts as the ^1H signals.

It is apparent from the NMR spectra that there is a fast equilibration of the porphyrin dimer to yield only two meso proton signals, two ring methyl signals, and so on, for each isomer. This fast equilibration is caused by one porphyrin macrocycle sliding over the other between two stable symmetry-related conformations (Figure 3(a)). This is the same effect as we have described in bipyridyl-bridged porphyrins.[8] Given the pattern of shifts observed in the major isomer, we may assign this as the meso compound since the stacking environment of the two porphyrins has

(12) (a) Anderson, C. J.; Hunter, B. K.; Leighton, P.; Raithby, P. R.; Sanders, J. K. M., in preparation. (b) Reference 11, Chapter 9.

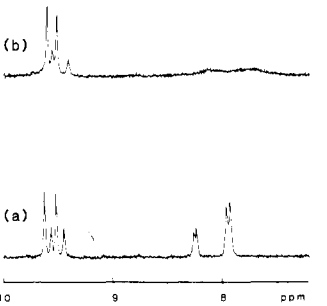

Figure 4. Meso region of the 400-MHz ^1H spectrum of **2** in 1,1,2,2-tetrachloroethane-d_2: (a) at 125 °C, (b) at 20 °C.

to be identical to produce the specific shift of just one methyl group or meso proton. The geometry of this isomer is discussed below.

The synthesis of the more tightly linked dimer **2** has been reported previously.[10b] This dimer too is formed as a mixture of two diastereoisomers; these we label syn and anti rather than meso and racemic because the unsymmetrical linking chain formally lifts the degeneracy of the two porphyrin macrocycles. The NMR spectra of **2** are, therefore, correspondingly more complex, but we show below that the two porphyrins are, in fact, in virtually identical environments.

Figure 4(a) shows the meso region of two ^1H spectra of **2** in 1,1,2,2-tetrachloroethane-d_2. At elevated temperatures, all the eight expected meso proton signals are resolved, falling clearly into two groups around 7.9–8.3 and 9.5–9.7 ppm. Thus the pattern observed in *meso*-**1** is repeated in both isomers of **2**. The possibility that all eight signals arise from a single isomer is precluded by the obvious intensity variation of the signals: again, we see an approximately 2:1 mixture. By analogy with *meso*-**1**, we assign the upfield group of meso proton signals to H_{20} and the less shifted group to H_5. The shift differences between the two nonequivalent porphyrins of an individual molecule are very small, and we have made no attempt to assign the signals in more detail.

At ambient temperature, the spectrum of **2** shows severe broadening of the most shifted signals (Figure 4(b)), presumably as a result of the same type of conformational equilibrium as we postulate in **1**. This cross-plane motion is illustrated in Figure 3(b). Further cooling of solutions of **2** failed to resolve the slow exchange spectrum.

Geometries of the Free-Base Dimers. Before discussing the quantitative aspects of geometry in detail, we can readily draw some qualitative conclusions. It is obvious that in *meso*-**1** the specific pattern of ring-current shifts suggests a well-defined, preferred geometry, whereas for the racemic isomer there is a general upfield shift with no pattern emerging. So it appears that this isomer has several conformational forms available and in fast exchange on the chemical shift time scale. The fact that there is no single preferred geometry suggests that there is no substantial energy minimum for the interporphyrin interaction in any available geometry.

The ring-current shifts for *meso*-**1** shown in Figure 2 were fitted to a best geometry by using the porphyrin ring current model as before.[8] The parameterization of the model and the limitations of the approach have been described in detail previously.[8] We simply stress here those considerations that are particularly relevant in these dimers. The room-temperature spectra of **1** reflect an average molecular symmetry, showing only two meso protons and two β-methyl signals. This is not the instantaneous symmetry, but rapid exchange between conformationally equivalent structures will result in the observed time-av-

Table I. Observed and Calculated Ring-Current Shifts in *meso*-1[a]

	shift			shift	
nucleus	obsd	calcd	nucleus	obsd	calcd
H_5	0.61	0.66	C_5	0.78	0.85
H_{10}	1.54	1.41	C_{10}	1.24	1.48
H_a	0.49	0.19	C_a	0.42	0.24
H_b	0.08	0.05	C_b	0.03	0.15
H_c	1.04	1.04	C_c	1.28	1.18
			C_d	1.33	1.65

[a] Upfield shifts are positive and relative to **5**.

Table II. Observed and Calculated Meso Proton Shifts in 2[a]

	major isomer		minor isomer	
proton	obsd	calcd	obsd	calcd
H_5	0.39, 0.51	0.11	0.43, 0.58	0.22
H_{10}	2.15, 2.18	2.02	1.79, 1.86	1.74

[a] In 1,1,2,2-tetrachloroethane-d_2 solution, 125 °C.

eraged spectrum; this is easily handled computationally, but it results in fewer data on which to perform an interaction and so leads to a less definitive geometry.

For the computations, the porphyrins were taken to be coplanar, with the same geometry and coordinate system as previously used,[8] and side chains were added with standard bond lengths and angles. Initially, the $\Delta\delta$ values for fixed protons were used to provide the dimer geometry. Dihedral angles of flexible side chains were then varied to minimize the agreement factor, AF. There is a twofold axis of symmetry relating the two moieties in the dimer, so the calculation reduces to the problem of calculating only one set of ring-current shifts, given the displacement coordinates of one porphyrin ring from the other. There are only three displacement coordinates, x, y, and z, and, for 1, always more than four observable shifts, so the solution is overdetermined. However, because the variation in ring current with distance is not particularly steep, the displacement coordinates are only reliable to ca. ±0.6 Å.

Calculations gave the coordinates of the center of one ring from the other as origin of x = 3.6 Å, y = 2.2 Å, z = 4.0 Å for the meso isomer. This geometry is shown in Figure 3(a). The root mean square (rms) error is 0.17 ppm, and the AF is 0.18. The 4-Å z separation corresponds approximately to porphyrin–porphyrin contact at the van der Waals radii (3.5 Å). Table I gives the observed and calculated shifts. As anticipated from the qualitative assessment of the ring-current shifts for the racemic compound, no reasonable fit to any single conformation was obtained for this molecule.

The geometry calculations for **2** are also less precise (Table II), in part at least because there are so few shifts available for fitting. The calculated displacement coordinates for the major isomer were x = 1.4 Å, y = 1.4 Å, z = 4.0 Å, while for the minor isomer they are 1.2, 1.2, and 4.2 Å respectively; these numbers give no guidance as to which isomer is syn and which anti. The geometry of the major isomer is illustrated in Figure 3(b); the minor isomer is very similar and is not shown.

Dimer Tetracations. Following protonation of 1 with deuteriated trifluoroacetic acid, to produce the tetracation, the ratio of diastereoisomers shifts, becoming approximately 3:2 in both dichloromethane and chloroform. Although it is not absolutely clear which diastereoisomer predominates, we presume that it is the meso isomer. The proton spectrum was readily assigned by a COSY experiment. The ring-current shifts, though still considerable, are now much smaller. The porphyrins are repelling each other, allowing the cavity size to be a maximum and thereby reducing the diastereoselectivity. Furthermore, all the meso proton resonances are now at similar chemical shift for both diastereoisomers (Table III). This indicates that they have similar geometries and that the offset stacking of the porphyrin rings seen in the neutral meso compound has been replaced, on average, by a direct face-to-face geometry as the two porphyrins repel each other but are restrained by the straps. The porphyrin–porphyrin separation is now about 9 Å.

Table III. Proton Ring-Current Shifts in Protonated Porphyrins[a]

compound	shifts, ppm
meso-1	0.49, 0.57
rac-1	0.38, 0.40
2	0.18–0.47[b]

[a] Relative to D_2-5^{2+} $2CF_3CO_2^-$, H_{meso} = 10.62, 10.57 ppm. [b] Individual signals are poorly resolved.

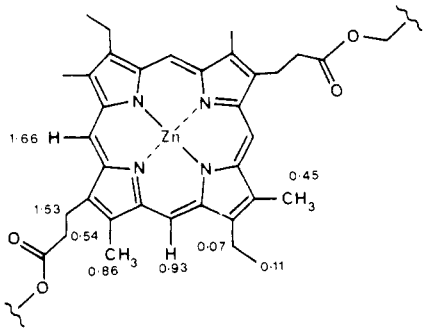

Figure 5. Upfield ring-current ^1H shifts in Zn_2-1.

Similar results are obtained for **2** (Table III), but there is no change in the isomer ratio on protonation. The cation spectrum is sharp because the cross-plane motions associated with the attractive π–π interactions are now absent.

Dizinc Dimers. The 250-MHz proton NMR spectrum of Zn_2-1 (not shown) shows that there is only one isomer present; we estimate the maximum amount of other isomer that may be present but avoid detection to be less than 2%. An inspection of chemical shifts suggests that this is the meso isomer, i.e., that which is dominant in the free base. This was confirmed by NOE difference spectroscopy, which showed that the spectrum was essentially the same as that of *meso*-1. From the assignment of the spectra, the ring-current shifts of all porphyrin resonances relative to Zn-**5** were deduced, and these are shown in Figure 5. It is worthy of note that the resonances in Zn_2-1 are remarkably sharp by comparison with zinc porphyrin monomers. Thus, while zinc monomers are aggregated in nonpolar solvents, this dimer is clearly not aggregated. Whatever the association demands leading to monomer aggregation may be, they are satisfied intramolecularly in Zn_2-1. It appears then that dimers such as Zn_2-1 are good models for metalloporphyrin aggregation. This idea is reinforced by the results of pyridine addition: the spectrum remains sharp, but the characteristic upfield shifts are reduced dramatically, implying a weakening of the porphyrin–porphyrin interaction. Ligand binding to Zn_2-1 and Zn_2-2 and its implications for the mechanism of porphyrin disaggregation by ligands will be discussed in detail elsewhere.[13]

Ring-current calculations analogous to those performed on the free base *meso*-1 yield a very similar structure for

(13) Leighton, P.; Hunter, C. A.; Cowan, J. A.; Sanders, J. K. M., in preparation.

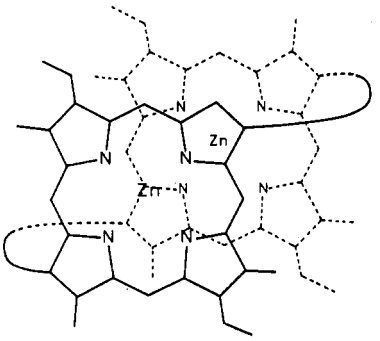

(a) High temperature

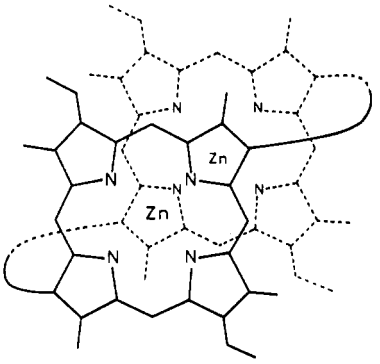

(b) Low temperature

Figure 6. High- and low-temperature calculated geometries for Zn_2-1.

Table IV. Observed and Calculated Ring-Current Shifts in Zn_2-1: High-Temperature Geometry[a]

	shift			shift	
proton	obsd	calcd	proton	obsd	calcd
H_5	0.93	0.87	H_b'	0.11	0.16
H_{10}	1.66	1.42	H_c	0.86	0.92
H_a	0.45	0.17	H_d	1.53	1.72
H_b	0.07	0.10	H_d'	0.54	0.99

[a] Relative to the pyridine adduct of Zn-5. Upfield shifts are positive.

Zn_2-1; the displacements are x = 3.0 Å, y = 2.0 Å, z = 4.0 Å. This fit gave an rms error of 0.23 ppm and an AF of 0.24. This structure is illustrated diagramatically in Figure 6(a), and the observed and calculated shifts are given in Table IV.

The ^1H resonances of Zn_2-1 are broader at 400 MHz than at 250 MHz, indicating an exchange process. Cooling a solution of Zn_2-1 in dichloromethane produces increased line broadening until at −30 °C the spectrum is so broad that no peaks are identifiable (Figure 7). At −90 °C the slow exchange limit is reached and four meso proton signals are clearly visible. The rest of the spectrum, with the exception of the methyl singlets, is not readily assignable since the simple multiplets of the strap are broad and complex due to both high solvent viscosity and the fact that the chains are now ordered so that the methylene protons are diastereotopic. The methyl and ethyl resonances are however well resolved, being dispersed over nearly 4 ppm. Addition of dichlorodifluoromethane in order to reduce the viscosity and give narrower lines caused precipitation of the porphyrin on cooling the solution to −100 °C.

The meso proton region is highly revealing: the two meso resonances at room temperature are at 9.2 and 8.4

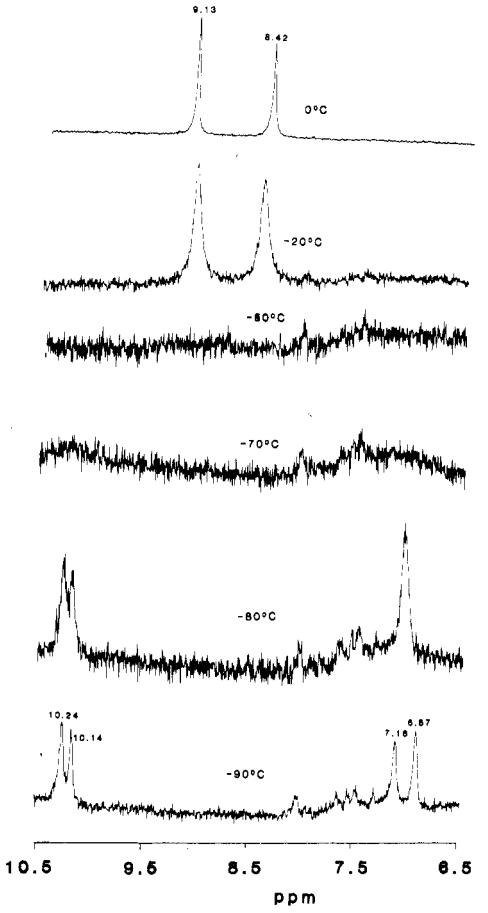

Figure 7. Part of the 400-MHz ^1H spectrum of Zn_2-1 in dichloromethane solution at various temperatures.

Table V. Observed and Calculated Ring-Current Shifts in Zn_2-1: Low-Temperature Geometry

	shifts[a]			shifts[a]	
proton	obsd	calcd	proton	obsd	calcd
H_5	2.94	2.84	H_b'	0.59	0.27
H_{10}	3.23	3.17	H_c	3.80	3.52
H_{15}	−0.04	−0.21	H_e	0.34	0.04
H_{20}	−0.14	−0.21	H_f'	0.11	0.00
H_a	−0.12	−0.23	H_g	−0.12	−0.18

[a] Upfield ring-current shifts are positive. H_e, H_f', and H_g are the methyl groups related through the porphyrin center of symmetry to H_a, H_b', and H_c respectively.

ppm, but the mid points of the meso proton signals observed at −90 °C are at ca. 8.5 and 8.7 ppm. This means that the high-temperature conformation is not simply an average of the low-temperature form. Either the preferred stacking conformation is temperature dependent or, at high temperatures, there is an equilibration of the low-temperature form plus an amount of some other, unspecified, form present. In order to attempt some distinction between these possibilities, we performed ring-current calculations by using the four low-temperature meso proton shifts. Crude geometries determined in this way allowed the assignment of all of the six methyl resonances. Then, using all of the 10 ring-current shifts thus determined, we determined the geometry of the low-temperature conformation. The best fit was obtained to a geometry where one porphyrin was displaced at x = 2.8 Å, y = 2.6 Å, z = 3.4 Å. This geometry, shown in Figure 6(b), gives an AF of 0.10 and an rms error of 0.18. The observed and calculated ring-current shifts are given in Table V.

Table VI. Observed and Calculated Meso Proton Shifts in Zn_2-2[a]

	major isomer		minor isomer	
	obsd	calcd	obsd	calcd
H_5	0.6, 0.7	0.11	0.6, 0.7	0.29
H_{10}	2.2, 2.3	2.02	1.8, 1.9	1.59

[a] In 1,1,2,2-tetrachloroethane-d_2 solution, 90 °C.

Warming a chloroform solution of Zn_2-1 to 50 °C produces very little change in the 250-MHz ^1H spectrum. The lines do not narrow significantly but remain rather broad (8 Hz for the methyl groups, 5 Hz for the meso signals). Hence this residual broadening must be due to the short correlation time caused by the slow tumbling of the molecule. There are also some slight shifts; in particular, the H_d' methylene moves slightly to high field of the overlapping methyl resonance in the room-temperature spectrum. Such changes have been observed in other bridged porphyrin systems[14] and have been interpreted as arising from a "breathing" of the bridge.

There are significant differences between the geometries determined at high and low temperatures for Zn_2-1. At low temperature there is increased overlap of the π systems and a decreased interannular separation. If the room-temperature spectrum is an equilibrium between more than two forms, we might expect further change in the spectrum to occur between −20 and 50 °C; however, little change is observed. This suggests, but does not prove, that the low-temperature conformation is indeed different from the two interconverting conformations observed above −20 °C.

The proton NMR spectrum of Zn_2-2 is broadened at ambient temperatures. On heating the sample to 90 °C in 1,1,2,2-tetachloroethane, we find that the spectrum sharpens and shows similar ring-current shifts on the meso resonances, and diastereoisomeric ratio, to those observed in the free base. This broadening may therefore again by ascribed to a dynamic process within the dimer, rather than to aggregation. Ring-current calculations carried out as above give the following geometries: for the major isomer, x = 1.4 Å, y = 1.4 Å, and z = 4.0 Å, while x = 1.0 Å, y = 1.0 Å, z = 4.2 for the minor isomer (Table VI). These geometries are almost identical with those of the free base and are not shown.

Absorption and Emission Spectra. The preceding NMR results clearly demonstrate *proximity* of the two porphyrin rings in these dimers; they also demonstrate that this proximity is dependent on metalation and coordination state. In this section we use electronic absorption and emission spectra to probe the *interaction* between the porphyrin rings.

The absorption spectrum of 1 (Table VII) shows a Soret band that is broadened, hypochromic, and hypsochromically shifted and Q bands that are hypochromic and bathochromically shifted, relative to 5. This is clearly the result of exciton coupling of the two chromophores.[9] Protonation with trifluoroacetic acid gives a spectrum (Table VII) that is now virtually identical with that of H_2-5^{2+}. Thus the two protonated porphyrins repel each other so much that there is no longer any significant exciton coupling between them. The degree of exciton coupling in 2 is very similar to that in 1, but protonation is less effective at abolishing it entirely (Table VII). Chromophore–chromophore interactions are also apparent in the red-shifted and somewhat quenched emission spectra of neutral 1 and 2 (Table VIII). As one might expect, fluorescence quenching in the protonated species is much less significant (Table VIII).

Both Zn_2-1 and Zn_2-2 have Soret absorbances that are broadened, hypsochromically shifted, and strongly hypochromic relative to Zn-5 (Table VII). Furthermore, both Zn_2-1 and Zn_2-2 show strongly shifted and quenched fluorescence relative to Zn-5.

Discussion

We divide this discussion into four sections: the local properties of the dimers 1 and 2 and their dizinc derivatives, the general question of the geometry of porphyrin–porphyrin interactions, the role of the zinc ion, and the use of these dimers as models for porphyrin aggregation and disaggregation.

Properties of the Dimers. Why is there weak diastereoselectivity in 1 itself, which has a meso:racemic ratio of 2:1, less selectivity in H_4-1^{4+} (3:2), and great selectivity (>50:1 in favor of meso) in Zn_2-1? The observation that there is reduced selectivity in the freshly prepared cation demonstrates that interconversion does take place on a time scale of minutes, even though it is slow on the saturation-transfer time scale in 1 itself. The quantitative yield of *meso*-Zn_2-1 from the isomeric mixture makes the same point. Undoubtedly the large interporphyrin distance in the cation and the associated lack of favorable interactions account for the lack of disastereoselectivity. By contrast, the selectivity in Zn_2-1 implies a stronger porphyrin–porphyrin interaction in the *meso* isomer than in 1. This is also apparent in the relative fluorescence properties of the two dimers (Table VIII).

Interconversion of the two stereoisomers requires rotation of one porphyrin through the cavity. CPK models reveal that this is difficult but possible in 1 and impossible in 2. Experimentally, this is confirmed by our observations that the isomer ratio in 2 is unchanged on metalation or protonation.

We have argued elsewhere[10a,c] that, in the macrocyclization reaction to make bridged or dimeric porphyrins, the formation of the second ester linkage is slow, being preceded by π–π complexation. If this were so, one would expect predominant formation of the thermodynamic product, and this certainly appears to be the case for 1, which has 10 linking atoms between porphyrins. It is not clear whether kinetic or thermodynamic factors dominate in the formation of 2 (seven linking atoms), while Collman reports that only the kinetically favored anti isomer is formed when a four-atom link is used.[15] Evidence for precyclization association of porphyrin and another π-system is apparent in the folded conformations described for porphyrins that are singly linked to anthraquinones.[16]

The Geometry of Porphyrin–Porphyrin Interaction. Each of the solution geometries determined in this work (other than the cations) demonstrates a low-symmetry, offset stacking rather than the face-to-face, maximum-symmetry, maximum-overlap stacking that might have been expected. Furthermore, *meso*-1 and Zn_2-1 have remarkably similar geometries as reflected in their characteristic meso proton chemical shifts. A search of published solution NMR data reveals that an almost identical pattern of shifts has been reported in many other dimeric porphyrin systems. Thus, we find virtually the same

(14) Ganesh, K. N.; Sanders, J. K. M.; Waterton, J. C. *J. Chem. Soc., Perkin Trans. 1* **1982**, 1617.

(15) (a) Collman, J. P.; Anson, F. C.; Barnes, C. E.; Bencosme, C. S.; Greiger, T.; Evitt, E. R.; Kreh, R. P.; Meier, K.; Pettmann, R. B. *J. Am. Chem. Soc.* **1983**, *105*, 2694. (b) Collman, J. P.; Bencosme, C. S.; Barnes, C. E.; Miller, B. D. *J. Am. Chem. Soc.* **1983**, *105*, 2704.

(16) Sanders, G. M.; van Dijk, M.; van Veldhuizen, A.; van der Plas, H. C. *J. Chem. Soc., Chem. Commun.* **1986**, 1311.

Table VII. UV/Visible Absorption Spectral Data of Porphyrins[a]

compound	λ_{max}, nm ($\epsilon \times 10^{-3}$) Soret	Q bands				FWHM,[b] nm
1	387 (182)	502 (18)	534 (12)	569 (9.2)	623 (6.0)	57
2	385 (192)	501 (18)	535 (12)	569 (9.6)	623 (6.2)	58
5	397 (164)	496 (13)	531 (10)	564 (6.8)	618 (4.5)	39
H_4-1^{4+}	401 (601)	549 (24)	592 (10)			14
H_4-2^{4+}	397 (610)	546 (21)	590 (12)			19
H_2-5^{2+}	401 (406)	547 (17)	591 (7.2)			12
Zn_2-1	388 (272)	537 (18)	572 (24)			28
Zn_2-2	388 (166)	534 (13)	577 (18)			31
Zn-5	402 (314)	530 (13)	568 (19)			13

[a] In dichloromethane solution. [b] Full width at half-height of the maximum absorbance of the Soret band.

Table VIII. Emission Properties of Porphyrins[a]

compd	λ_{em}, nm	ϕ_f (rel)[b]
1	626	0.47
2	624	0.54
5	621	1.0
H_4-1^{4+}	598	0.79
H_4-2^{4+}	596	0.71
H_2-5^{2+}	596	1.0
Zn_2-1	586	0.15
Zn_2-2	570	0.20
Zn-5	572	1.0

[a] Recorded in dichloromethane solution at concentrations of ca. 10^{-6} M with irradiation at the Soret maximum. [b] Fluorescence emission per porphyrin moiety, relative to 5, H_2-5^{2+}, or Zn-5 as appropriate.

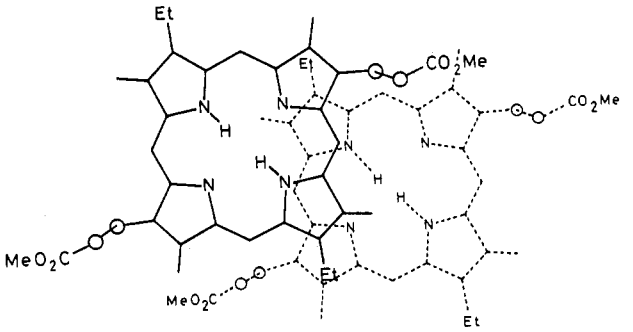

Figure 8. Relationship between individual molecules of 5 in the crystal (P. R. Raithby, unpublished).

chemical shifts reported in a doubly bridged porphyrin,[17] in a tightly linked porphyrin dimer,[18] and in a dimer linked by two flexible crown ether groups.[19] Given the large range of symmetry and linkage types in these different series of dimers, we conclude that the recurrent solution geometry is more fundamental than one imposed by purely local considerations such as strain. Indeed, CPK models of 1 appear to fall into the proposed geometry with no strain whatever.

Support for the generality of this type of geometrical motif is provided by several additional, independent lines of evidence.[3-7] For example, aggregates of zinc mono- and dinitrooctaethylporphyrins and zinc protoporphyrin IX dimethyl diester show NMR ring-current shifts that have been interpreted in terms of geometries that are similar to the low-temperature form of Zn_2-1.[6,20] ESR studies of dicopper porphyrin dimers lead to the same conclusion:[5] a porphyrin–porphyrin distance of 3.9 Å and a metal–metal distance of around 6 Å are found in the longer chained dimers, once again demonstrating the presence of an offset geometry. Furthermore, variable-temperature ESR measurements on Cu_2-2 reveal a shift to a less offset geometry on cooling,[21] closely mirroring our NMR results.

Finally, offset geometries have been found in the crystal structures of two dicopper dimers[7,21] and monomeric 5 itself.[12] In Chang's structure, which is effectively the amide analogue of Cu_2-2, it is noteworthy both that only the meso form is isolated and that, in the crystal, the intra- and intermolecular relationships of adjacent porphyrins are very similar to our solution geometry for 1. This evidence that the restraints of connecting chains are not important is further supported by the crystal structure of 5.[12] Figure 8 shows the relationship between two molecules of 5 in adjacent crystal planes. The coordinates of the center of one molecule with respect to the next are x = 5.2 Å, y = −1.9 Å, z = 3.4 Å. The differences between this crystal geometry and that of *meso*-1 in solution are relatively minor, amounting only to an additional x offset of 1.6 Å. As a further check on our NMR methodology, we have assigned the CPMAS ^{13}C spectrum of crystalline 5 and find precisely the pattern of shifts in the protonated carbons that would be predicted from the crystal structure.[12]

Our studies on 2 and Zn_2-2 and other work on tightly linked dimers[5,15,23] indicate that they take up less offset geometries. This may be a simple consequence of the bond strain that would be associated with such geometries.

One uncertainty remains. What is the nature of the attractive interactions between porphyrins? Preliminary (unpublished) calculations indicate that the experimentally observed geometry may be that which maximizes favorable electrostatic interactions between the π-systems; however, more sophisticated molecular orbital calculations will be required to confirm this.

The Role of Zinc. It seems clear from our results that the central zinc ion may modulate the strength of porphyrin–porphyrin interactions, but it does not fundamentally alter them. This is apparent in the almost coincident geometries of *meso*-1 and high-temperature Zn_2-1 and in the influence of pyridine coordination. The very small binding constant for pyridine, ca. 100 L mol^{-1} per porphyrin face,[13] corresponds to $\Delta G \sim 11.5$ kJ mol^{-1}. This should be compared with 24.5 kJ mol^{-1} for Zn-5 and suggests that the π–π interaction in Zn_2-1 is worth ca. 13 kJ mol^{-1} per porphyrin.

Dimers as Models for Aggregation. One of the most striking observations in this work is that these dimers do

(17) Cowan, J. A.; Sanders, J. K. M.; Beddard, G. S.; Harrison, R. J. *J. Chem. Soc., Chem. Commun.* **1987**, 55.
(18) Dubowchik, G.; Hamilton, A. D. *J. Chem. Soc., Chem. Commun.* **1986**, 665.
(19) Hamilton, A. D.; Lehn, J.-M.; Seseler, J. L. *J. Am. Chem. Soc.* **1986**, *108*, 5158.
(20) Abraham, R. J.; Fell, S. C. M.; Pearson, H.; Smith, K. M. *Tetrahedron* **1979**, *35*, 1759.
(21) Cowan, J. A. *J. Chem. Soc., Dalton Trans.*, in press.
(22) Collman, J. P.; Chong, A. O.; Jameson, G. B.; Oakley, R. T.; Rose, R.; Schmitton, E. R.; Ibers, J. A. *J. Am. Chem. Soc.* **1981**, *103*, 516.
(23) Fillers, J. P.; Ravichandran, K. G.; Abdalmuhdi, I.; Chang, C. K. *J. Am. Chem. Soc.* **1986**, *108*, 417.

not aggregate at NMR concentrations ($\sim 10^{-3}$ M). This behavior contrasts markedly with that of monomeric porphyrins, Zn-**5** being strongly aggregated at NMR concentrations. Zn-**5** is apparently disaggregated at UV concentrations (10^{-5}–10^{-6} M), to judge by the lack of exciton coupling. We can conclude, therefore, that the major driving force in porphyrin aggregation is satisfied by a single π–π stacking on one side to give dimers; further oligomerization is a much weaker process.

In our dimers, pyridine ligation on one face can decrease or abolish π–π interaction at the other face of the porphyrin.[13] Similarly, addition of a ligand such as pyridine breaks up aggregates to give monomeric products of 5-coordinate zinc porphyrins. Despite the fact that these ligated porphyrins have one unhindered face, they do not dimerize, since the coordinative unsaturation of the system has been satisfied. On the basis of this evidence, we conclude that our dimers are indeed good models of porphyrin–porphyrin aggregation.

Experimental Section

General synthetic directions have been presented previously.[10] ^{1}H NMR spectra were obtained at 250 or 400 MHz on Bruker WM250 or WH400 instruments; the same spectrometers provided ^{13}C spectra at 62.6 or 100 MHz. NOE difference, COSY, and ^{1}H–^{13}C correlation experiments were carried out with standard software and pulse sequences.[11] Details of titration procedures and ring current shift calculations were as previously described.[8] Emission spectra were recorded by using a Perkin-Elmer 3000 fluorescence spectrometer.

Mesoporphyrin II–Bis(ethane-1,2-diol) Diester (4). Mesoporphyrin II (300 mg, 0.63 mmol) was converted into the bis(acid chloride) **3** as described previously.[10] The bis(acid chloride) was taken up into dry dichloromethane (75 mL), and a mixture of dry pyridine (2 mL) and dry freshly distilled ethylene glycol (3 mL) was added; a vigorous reaction occurred. Water (100 mL) was added, and the organic layer was extracted. The organic layer was dried and the solvent removed. The residual pyridine was removed under high vacuum. The residue was taken up into dichloromethane (2 mL) and chromatographed by preparative TLC over silica gel (eluant dichloromethane–5% methanol). Recrystallization from dichloromethane–hexane gave the diol as a purple solid: yield 150 mg (43%); mp 265–267 °C; ^{1}H NMR (250 MHz, $CDCl_3$ + TFA-*d*) δ 10.73 (2 H, s, meso), 10.60 (2 H, s, meso), 4.44 (4 H, t, J = 7 Hz, H_d), 4.09 (4 H, q, J = 7 Hz, H_b), 3.89 (4 H, t, J = 5 Hz, CH_2OCO), 3.63 (6 H, s, porphyrin methyl), 3.65 (6 H, s, porphyrin methyl), 3.20 (4 H, t, J = 5 Hz, CH_2O), 3.15 (4 H, t, J = 7 Hz, H_d'), 1.76 (6 H, t, J = 7 Hz, H_b').

Bis(mesoporphyrin II–ethane-1,2-diol) Cyclic Tetraester (1). By the macrocyclization procedure outlined above, mesoporphyrin II bis(acid chloride) (0.46 mmol) was reacted with mesoporphyrin II–bis(ethane-1,2-diol) diester (300 mg, 0.46 mmol) to give **1** (54 mg, 9.7%) as fine purple crystals from dichloromethane–hexane: mp >300 °C; ^{1}H NMR (250 MHz, $CDCl_3$) meso isomer δ 9.45 (4 H, s, H_5), 8.51 (4 H, s, H_{10}), 4.21 (8 H, s, CH_2O), 4.0 (8 H, q, J = 7 Hz, H_b), 3.19 (12 H, s, H_a), 2.54 (12 H, H_c), 2.46 (8 H, t, J = 7 Hz, H_d), 2.22 (8 H, t, J = 7 Hz, H_d'), 1.89 (12 H, t, J = 7 Hz, H_b'), racemic isomer δ 9.45 (4 H, s, meso), 9.41 (4 H, s, meso), 4.10 (8 H, s, CH_2O), 3.56 (8 H, t, J = 7 Hz, H_d), 3.47 (8 H, q, J = 7 Hz, H_b), 3.14 (12 H, s, porphyrin methyl), 2.98 (12 H, s, porphyrin methyl), 2.64 (8 H, t, J = 7 Hz, H_d'), 1.47 (12 H, t, J = 7 Hz, H_b'); ^{13}C NMR ($CDCl_3$) *meso*-**1** δ 172.79 (C_d''), 141.09, 137.92, 135.14, 134.21, ($C_{2,3,7,8}$), 95.66 (C_5), 95.03 (C_{10}), 62.23 (CH_2O), 36.71 (C_d), 20.68 (C_b), 19.81 (C_d'), 17.70 (C_b'), 11.07 (C_a), 10.47 (C_c), *rac*-**1** δ 172.68 (C_d''), 140.90, 138.31, 136.62, 133.88 ($C_{2,3,7,8}$), 95.96 (C_5), 95.75 (C_{10}), 62.08 (CH_2O), 36.77 (C_d), 21.33 (C_b), 19.28 (C_d'), 17.21 (C_b'), 11.13 (C_c), 10.98 (C_a); FAB MS, m/e 1184 (M^+); Anal. Found: C, 71.25%; H, 7.14%; N, 9.03%, $C_{72}H_{80}N_8O_8 \cdot 2H_2O$ requires C, 70.86%, H, 6.89%; N, 9.19%.

***meso*-D_4-1^{4+}**: ^{1}H NMR (250 MHz, CD_2Cl_2 + TFA-*d*) δ 10.25 (4 H, s, meso), 10.17 (4 H, s, meso), 4.28 (8 H, t, J = 7 Hz, H_d), 4.07 (8 H, s, CH_2O), 3.97 (8 H, q, J = 7 Hz, H_b), 3.51 (12 H, s, porphyrin methyl), 3.40 (12 H, s, porphyrin methyl), 2.59 (8 H, t, J = 7 Hz, H_d'), 1.56 (12 H, t, J = 7 Hz, H_b').

***rac*-D_4-1^{4+}**: ^{1}H NMR (250 MHz, CD_2Cl_2 + TFA-*d*) δ 10.13 (4 H, s, meso), 10.00 (4 H, s, meso), 4.41 (8 H, t, J = 7 Hz, H_d), 4.31 (8 H, s, CH_2O), 3.97 (8 H, q, J = 7 Hz, H_b), 3.51 (12 H, s, porphyrin methyl), 3.50 (12 H, s, porphyrin methyl), 2.96 (8 H, t, J = 7 Hz, H_d'), 1.56 (8 H, t, H_b').

Bis(zinc mesoporphyrin II–ethane-1,2-diol) Cyclic Tetraester (Zn_2-1). By the usual metalation procedure,[10] free base **1** (10 mg) was converted into Zn_2-**1**. Recrystallization from dichloromethane–pentane gave bright red microcrystals: yield 11 mg (100%).

When crystalline, Zn_2-**1** was poorly soluble in dichloromethane, requiring ultrasonic agitation to dissolve a reasonable amount. Alternatively, a more soluble amorphous form could be prepared by dissolving the crystalline material in dichloromethane–5% pyridine, in which it was more readily soluble, and extracting the pyridine by shaking with copper sulfate solution (2 × 75 mL). After washing with water (2 × 50 mL), drying, and evaporation of the solvent under reduced pressure, a readily soluble form of the dimer was obtained. Proton NMR and UV/visible spectroscopy verified the total removal of pyridine: ^{1}H NMR (250 MHz, CD_2Cl_2, 20 °C) δ 9.17 (4 H, s, H_5), 8.42 (4 H, s, H_{10}), 4.48 (8 H, s, CH_2O), 4.02 (8 H, q, J = 7 Hz, H_b), 3.17 (12 H, s, H_a), 2.76 (12 H, s, H_c), 2.93 (8 H, t, J = 6 Hz, H_d), 2.72 (8 H, t, J = 6 Hz, H_d'), 1.78 (12 H, t, J = 7 Hz, H_b'), (250 MHz, CD_2Cl_2–pyridine-d_5) δ 9.67 (4 H, s, H_5), 9.43 (4 H, s, H_{10}), 3.83, (8 H, s, CH_2O), 3.38 (12 H, s, H_a), 3.11 (12 H, s, H_c), 3.63 (8 H, t, J = 7 Hz, H_d), 2.71 (8 H, t, J = 7 Hz, H_d'), 1.75 (12 H, t, J = 7 Hz, H_b').

Acknowledgment. We thank C. Sporikou for the supply of **5** and the SERC and St John's College, Cambridge, for Studentships (J.A.C., P.L.). We are indebted to P. R. Raithby for carrying out the X-ray crystal structure study of **5** and to C. A. Hunter for some of the fluorescence measurements.

Registry No. **1** (meso), 112271-03-1; **1** (roc), 112345-65-0; 1_{D4}^{4+} (meso), 112346-54-0; 1_{D4}^{4+} (roc), 112345-66-1; Zn_2-**1** (meso), 112271-07-5; **2** (syn), 110840-04-5; **2** (anti), 112345-67-2; **3**, 112271-05-3; **4**, 112271-06-4; **5**, 112296-50-1; mesoporphyrin-II, 69423-12-7.